International Journal of Disaster Risk Reduction 101 (2024) 104193

Contents lists available at ScienceDirect

International Journal of Disaster Risk Reduction

journal homepage: www.elsevier.com/locate/ijdrr

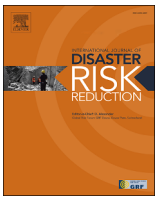

Integrated tsunami risk framework considering agent-based evacuation modelling: The case of Saga, Kochi Prefecture, Japan

Ario Muhammad [a, b], Raffaele De Risi [b], Flavia De Luca [b, *], Widjo Kongko [a], Nobuhito Mori [c], Tomohiro Yasuda [d], Katsuichiro Goda [e, f]

[a] Hydrodynamic Technology Research Center, National Research and Innovation Agency Indonesia, Surabaya, Indonesia
[b] Department of Civil Engineering, University of Bristol, Bristol, UK
[c] Disaster Prevention Research Institute, Kyoto University, Kyoto, Japan
[d] Kansai University, Osaka, Japan
[e] Department of Earth Sciences, Western University, London, Canada
[f] Department of Statistical & Actuarial Sciences, Western University, London, Canada

A B S T R A C T

This study develops an integrated tsunami risk framework combining stochastic tsunami hazard and agent-based evacuation modelling. The framework is applied to the case of Saga, Kochi, Japan, with a population of ~ 2,200 anticipated to experience significant tsunami events (~ M9.0). First, stochastic earthquake source models are generated for two values of magnitudes (M8.8 and M9.0) and used to carry out stochastic tsunami inundation simulations. Agent-based tsunami evacuation modelling using MATSim is then performed by considering four mode scenarios: single mode (pedestrian and car) and two multimodal scenarios (mix of car and pedestrian). The stochastic tsunami simulations and agent-based evacuation modelling results are integrated to estimate the risk. The effect of existing tsunami evacuation points and tsunami evacuation towers on risk reduction is also assessed. Such an integration framework is finally used to recommend tsunami mitigation strategies in the tsunami-prone regions. Results show that a significant tsunami hazard (i.e., tsunami depth up to 15 m) is expected in the Saga district, with an arrival time between 5 and 30 min. In addition, the evacuation points on higher grounds effectively save local residents' lives, as shown by the small number of affected people, specifically for the pedestrian and multimodal models (i.e. 10-100 people, excluding the car model). However, up to ~ 1,000 people may get affected if car is the sole mode of evacuation. Therefore, the coastal community is recommended to evacuate on foot. Finally, identifying and securing sufficient higher grounds and vertical evacuation points are essential for risk reduction.

1. Introduction

In the last two decades, tsunamis have been the most devastating natural disaster in the world, causing fatalities exceeding 200,000 people and economic losses of more than 14,000 billion USD [1]; [2]. A current trend for assessing tsunami hazards involves adopting a probabilistic tsunami hazard analysis framework. For instance, stochastic earthquake source models have been developed to capture the uncertainty of future tsunami hazards in tsunami-prone regions, i.e., Mexico, Japan, and Indonesia [3–5 6] [7]. Such stochastic tsunami simulation results have been used to quantify the tsunami risks [8][9]. Moreover, developing effective tsunami evacuation plans is one of the important actions to reduce fatality risks in the future. In general, evacuation plans have been developed using static and dynamic approaches. The static approach does not need detailed transportation networks and evacuees' features, leading to unrealistic evacuation plans. In contrast, the dynamic approach (i.e., agent-based evacuation method) produces a more realistic evacuation plan because it uses detailed features of transportation infrastructure, agents' movements, and potential interaction among the agents [10,11].

* Corresponding author.
E-mail address: flavia.deluca@bristol.ac.uk (F. De Luca).

https://doi.org/10.1016/j.ijdrr.2023.104193
Received 18 February 2023; Received in revised form 8 December 2023; Accepted 9 December 2023
Available online 15 December 2023

Several studies carried out single-mode and multimodal agent-based tsunami evacuation simulations using software such as MATSim or NetLogo [12,13,14,15, 16] by mainly focusing on simulation parameters, such as the optimized iteration number and traffic flow. However, a more realistic multimodal scenario needs to be developed extensively. Moreover, those multimodal evacuation studies have not included rigorous hazard simulations considering the uncertainty of future tsunamigenic events in the evacuation framework ([13–16] [;). In these previous studies, tsunami evacuation points were selected deterministically and assigned to high grounds (i.e., >10 m) without a comprehensive assessment of possible inundation scenarios in a region of interest [12]. In a recent study, an agent-based tsunami evacuation model has been developed to consider the uncertainty of future tsunami hazards integrating evacuation using stochastic inundation maps generated from the source models of the Mentawai-Sunda subduction zone [17]. However, only a single-mode evacuation modelling of pedestrians or motorbikes was adopted without considering the multimodal approach. Moreover, this study performs a rigorous evaluation of evacuation simulation parameters (i.e., number of iterations and queueing model choice), which has not been carried out by [17] before running the simulation.

Among the tsunami-prone regions globally, the Saga district in Kochi Prefecture, Japan, is expected to experience significant tsunamigenic earthquakes from the Nankai-Tonankai subduction zone. The Saga district is located in front of the Nankai-Tonankai subduction zone; therefore, a tsunami height of more than 20 m may arrive at the coast (Fig. 1a; [18] [19] [7,9]. Rigorous probabilistic tsunami hazard analysis was carried out in this region before this work and produced detailed information on possible tsunami hazard data (e.g., tsunami height, inundated areas, and tsunami arrival time; [7,9]. The Central Disaster Management Council of Japan [18] has also released the tsunami hazard map and evacuation plan for the Saga district due to the future Nankai-Tonankai subduction earthquakes (Fig. 1b) [20]. Moreover, after the 2011 Tohoku tsunami, new vertical tsunami evacuation towers (TET) were built in Saga to reduce fatalities, and detailed population and network data to develop realistic evacuation modelling are available. Furthermore, integrating the probabilistic tsunami hazard data from [7,9] with the agent-based evacuation results (i.e., tsunami evacuation time) allows the estimation of casualty risk in terms of the number of affected people (i.e., people unable to evacuate, being caught by the waves).

Subsequently, this study aims to develop an integrated tsunami risk probabilistic framework considering stochastic tsunami hazard and agent-based evacuation modelling by adopting the Saga district in Kuroshio Town, Kochi Prefecture, Japan, as a case study. This research is truly interdisciplinary because several methodologies have been used to create a comprehensive framework involving stochastic tsunami hazard, exposure, risk, and agent-based evacuation modelling. Specifically, the proposed method includes (1) developing probabilistic/stochastic tsunamigenic source models [21,22], (2) conducting probabilistic tsunami hazard and risk assessments [3,8,23 [[19]7,9], and (3) modelling probabilistic agent-based tsunami evacuation [17]. Agent-based evacuation modelling using MATSim requires the location of agents and the identification of links and nodes within a transportation network. Hence, developing realistic agents (i.e., population) and network data in the area of interest is essential. With respect to previous studies, this research adopts a multimodal scenario (i.e., mixed traffic of cars and pedestrians) to carry out agent-based evacuation modelling that has not been carried out in previous works [12–14,17]. This study can also evaluate the current existing horizontal evacuation plan (i.e. local higher grounds and vertical shelter) in saving residents and may offer sound recommendations for the local stakeholders to prepare the coastal communities against future tsunamigenic events.

This paper builds on insights obtained from our previous publication, i.e., [17], regarding agent-based simulation. More specifically, the previous paper mainly focused on defining agent-based evacuation simulation parameters, whereas this paper aims to integrate the stochastic tsunami hazard and agent-based evacuation simulation to generate a new integrated framework for casualty risk assessment. Therefore, the paper is organized as follows. First, the developed integrated framework is presented (Section 2.1). Second, the stochastic tsunami hazard is discussed (Section 2.2). Third, the approach to carrying out the agent-based tsunami evacuation modelling is presented (Section 2.3). Fourth, the approach to calculating the risk in terms of the number of affected people is explained (Section 2.4). Fifth, the results are presented, discussed (Section 3), and then used to develop recommendations for tsunami mitigation strategies (Section 4).

2. Methodology

2.1. Integrated framework

This study incorporates several methodologies to develop the integrated framework for casualty risk assessment (Fig. 2). Initially, a stochastic tsunami hazard analysis is conducted to estimate the tsunami hazard in a region of interest (Fig. 2a). Two essential steps

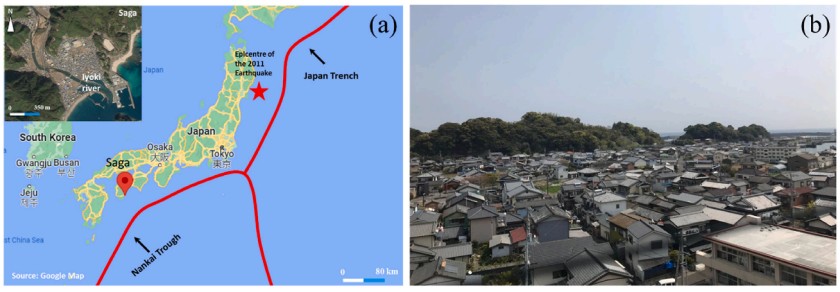

Fig. 1. (a) Study area, Saga district in Kochi Prefecture, Japan and (b) Top view of houses in Saga.

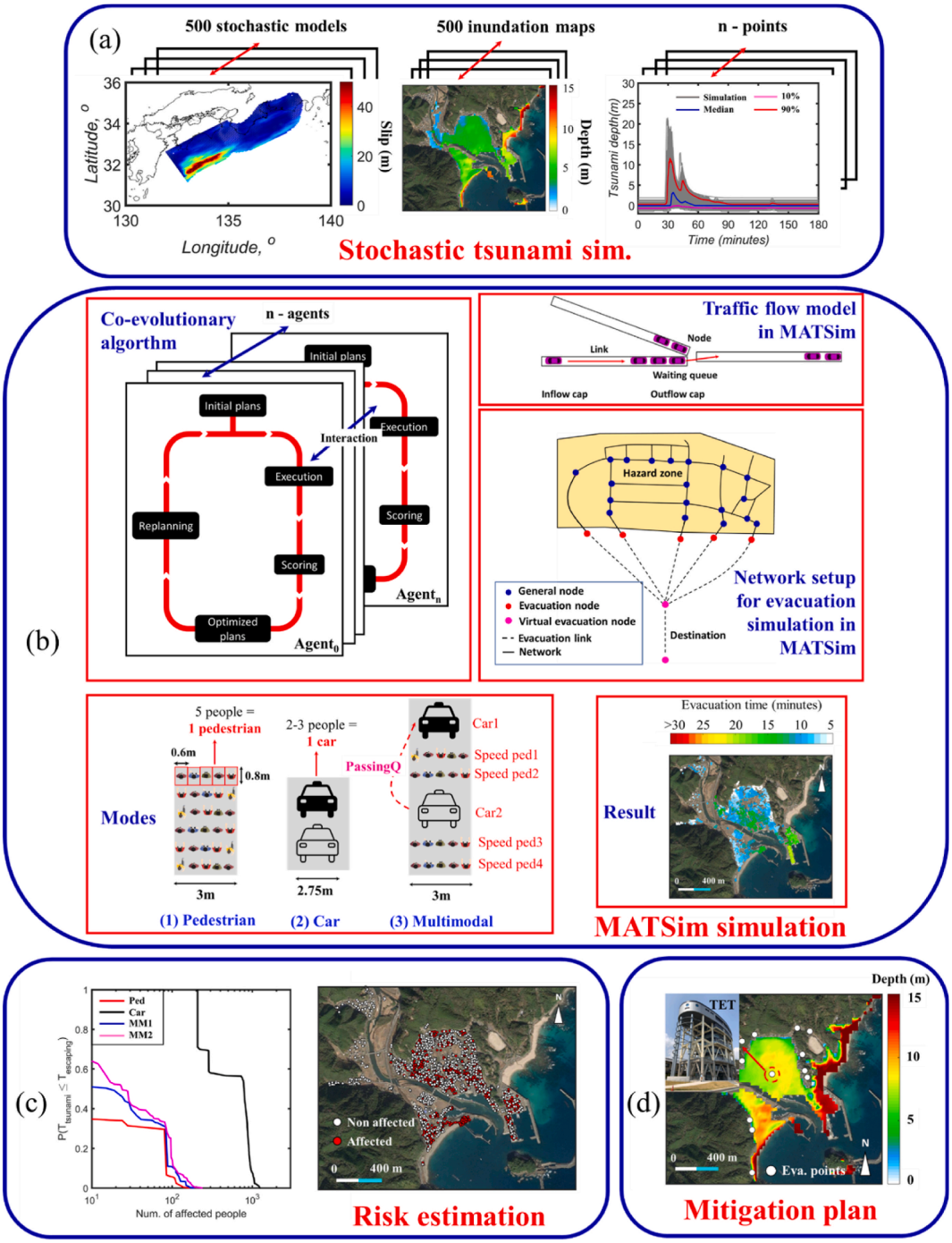

Fig. 2. Integrated framework for tsunami casualty risk assessment: (a) stochastic tsunami simulation, (b) tsunami evacuation modelling using MATSim, (c) casualty risk estimation, and (d) development of mitigation plan.

for the stochastic tsunami hazard analysis are (1) the generation of stochastic earthquake source models and (2) the stochastic tsunami simulation. Two magnitude values (i.e., M8.8 and M9.0) are adopted to generate the source models with a total of 1,000 cases (i.e., 500 for each magnitude value; Fig. 2a). Uncertainties and dependencies among source parameters (e.g., source geometry and slip) are considered in generating stochastic earthquake sources through Monte Carlo simulations. The tsunami simulations are then performed for each source model. Several hazard parameters, including stochastic inundation maps (Fig. 2a) and tsunami arrival times at road networks, are obtained from the stochastic simulations (Fig. 2a). In Fig. 2, *n* represents the number of nodal points where tsunami arrival times are recorded.

In this study, detailed evacuation networks and several modes of transportation (e.g., single and multimodal, MM) are considered to simulate a realistic evacuation plan. The agent-based evacuation is modelled using MATSim (Fig. 3b). The evacuation characteristics, such as (1) the evacuation duration, (2) critical agents/areas, and (3) critical infrastructures/links, can be identified based on the results of the agent-based evacuation modelling. The evacuation time computed with the agent-based evacuation modelling (Fig. 2b) and the tsunami arrival time calculated from the stochastic tsunami simulations (Fig. 2a) are combined to calculate the number of affected people (i.e., casualty assessment, Fig. 2c). Finally, reliable mitigation strategies (e.g., developing evacuation plans; Fig. 2d) can be proposed to the local stakeholders. A detailed description of each approach adopted in this study is presented in the subsequent sections.

2.2. Stochastic tsunami hazard simulations

The tsunami hazard in the region of interest is estimated using stochastic tsunami simulations. The stochastic earthquake source models are first generated in the stochastic tsunami simulations by considering the uncertainty and dependency of earthquake source parameters (Fig. 3a). In this study, the stochastic earthquake source models for two magnitude scenarios (i.e., M8.8 and M9.0) are generated from the Nankai-Tonankai megathrust areas in Japan. Such magnitude scenarios are adopted based on the proposed future tsunamigenic events by the [20]. The 2012 CDMC 2D fault plane model from the Japanese Cabinet Office is used as a baseline for generating stochastic models. The dimension of the sub-faults strike and dip angles is 5 km by 5 km, reflecting the current tectonic setting in the Nankai-Tonankai Trough region [24], and the sizes of matrix along-strike and down-dip directions are 153 and 53, respectively.

Furthermore, the scaling relationships of [22] are adopted to sample earthquake source parameters. Those parameters include the size (length, L and width, W), slip (mean, D_a and maximum slip, D_m), and other statistical parameters (i.e. Hurst number, H, Box-Cox parameter λ, correlation length along strike direction, A_x, and correlation length along dip direction A_z). These scaling relationships

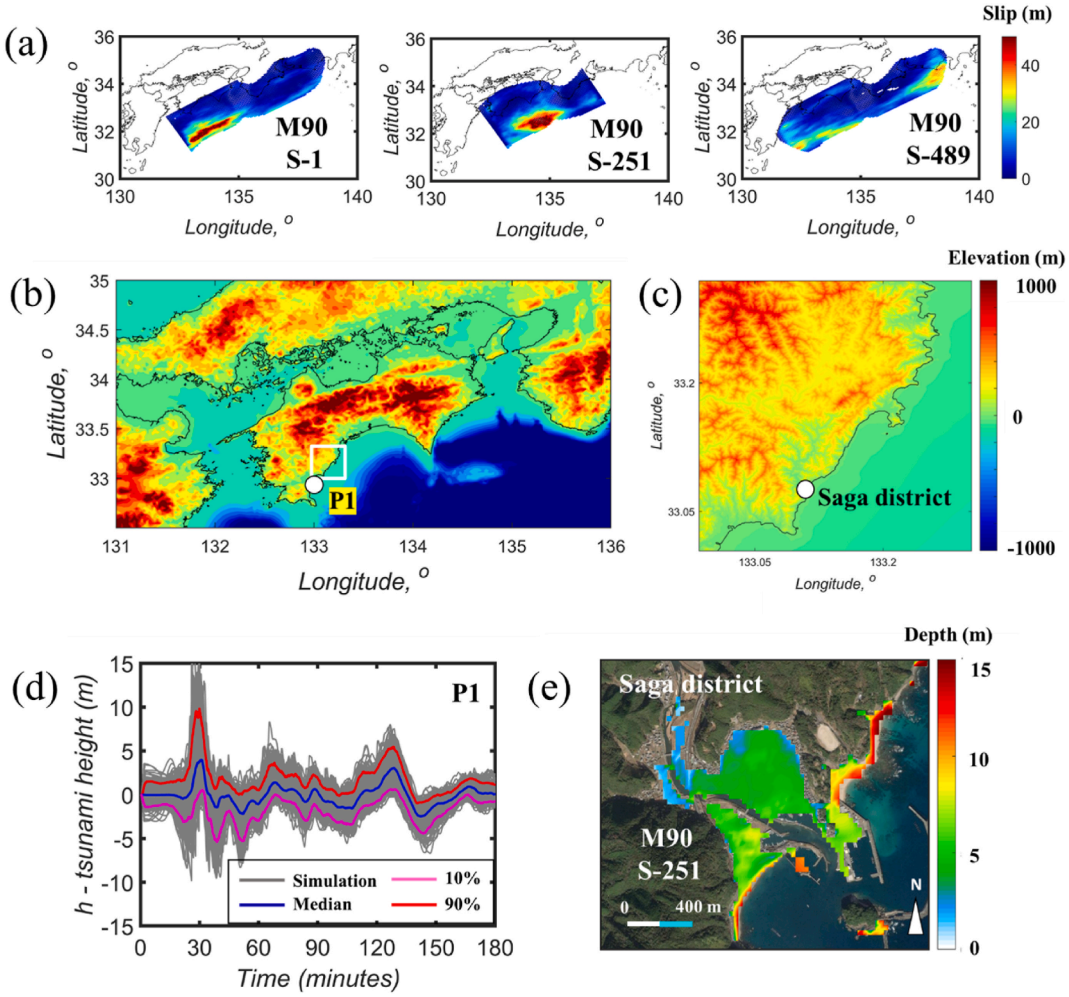

Fig. 3. (a) Stochastic source models - scenarios 1, 251, and 489. (b–c) DEM and Bathymetry data. (d) Tsunami wave height profiles. (e) Tsunami inundation maps - scenario 251, M9.0 case.

are developed based on the existing inversion source models of the major earthquakes [25]. The generated source parameters are evaluated to confirm their consistency by iteratively sampling the parameters of L, W, and D_a from the source scaling relationships until it has ± 0.1 magnitude units of the target moment. Adding μ as the rock rigidity, such target moment is calculated using $M_o = \mu WLD_a$. Finally, the earthquake source models from the two magnitude cases, i.e. M8.8 and M9.0, are generated with a total of 1,000 stochastic models (i.e., 500 models each). Such a number of stochastic models is adequate to produce consistent tsunami hazards [26].

Tsunami simulations are then performed using the generated earthquake source models, focusing on the Saga district. Elevations, bathymetry, coastal/riverside structures (e.g., breakwater and levees), and surface roughness data are needed to construct the tsunami simulation grid (Fig. 3b and c). The 5-m DEM, bathymetry, and coastal structure data are taken from the Geospatial Information Authority of Japan, the Japan Hydrographic Association, and the national coastline database, respectively. Those data are further adopted and nested following a 1/3 nesting ratio rule, i.e., 2430-m – 810-m – 270-m – 90-m – 30-m for tsunami simulations. In this study, the local onshore inundation modelling in Saga, where the tsunami evacuation tower exists, focuses on a grid system of 30 m (Fig. 3c).

The initial water surface elevation is further calculated using [27,28] equations, and tsunami waves are propagated using the [29] model. Manning's bottom friction coefficients are based on national land use data in Japan, i.e., 0.02 $m^{-1/3}s$, 0.025 $m^{-1/3}s$, 0.03 $m^{-1/3}s$, and 0.04 $m^{-1/3}s$ for agricultural land, ocean/water, forest vegetation, and residential areas, respectively. Adopting the kinematic fault rupture process (see [7,19] for the details), the tsunami simulation is carried out with a duration and time step of 3 h and 0.5 s, respectively, by satisfying the Courant-Friedrichs-Lewys criterion [30]. Finally, the Monte Carlo simulation is carried out, and their results in terms of tsunami inundation maps, wave height, and arrival times are evaluated (Fig. 3d and e).

2.3. Agent-based tsunami evacuation modelling

A microscopic traffic modelling software MATSim is used to run the agent-based evacuation modelling. MATSim simulates the movements of people based on their journeys with pre-defined plans using a co-evolutionary algorithm. Such an algorithm produces an optimized final plan conducted by simulating iteratively based on the score representing the agent's utility in terms of distance and time needed to reach their final destinations [31,32]. Therefore, the final evacuation plan is remarkably close to an ideal situation. Such an approach is suitable for our case study area (i.e., Kuroshio, Japan) as the evacuation drilling is conducted regularly and the evacuation infrastructure is well built.

The iteration number and the movement strategy are first determined to perform the agent-based tsunami evacuation. In this study, the number of iterations is fixed equal to 1,000 for the simple case (single mode) and 5,000 for complex cases (multimodal). The movement strategy is set up with the following assumptions: (1) 10 % of *Reroute* to generate a new movement plan based on the past experience of the agents and (2) 90 % of *BestScore* to execute a new plan based on the best score up to the current iteration. The score, *U,* in the MATSim simulation, is a function of distance and time [12]:

$$U_i = \left(\beta_{tr} \times t_{tr}\right)_i + \left(\beta_{dis} \times d\right)_i \quad (1)$$

where β_{tr} and β_{dis} are the utility parameters for time to travel (t_{tr}) and distance (d), respectively. β_{tr} can be negative to represent a situation where the agent is travelling and not improving the evacuation duration. Consequently, the simulated scores may be negative.

Three aspects are needed to model the movement of the agents in MATSim: links, nodes, and modes. Link and nodes are defined by the road network, whereas modes are defined based on pre-defined plans. In addition, the number of agents depends on the population data in the study areas. In this study, the links and nodes are developed based on the network infrastructure data in the Saga district (see Fig. 4a), i.e., ~ 170 nodes are used to connect ~ 330 links (more details are provided in [17]. For the evacuation simulation purpose, the maximum traffic flow speed is restricted, i.e., 2 m/s and 8.3 m/s for pedestrians and cars, respectively [8,33]. The pedestrian speed in the simulation changes depending on the slope of the corresponding links and thus is updated accordingly depending on the agent's position and the terrain topography. The hiking function of Toblers is used to calculate the change in pedestrian speed [34]. Using these speed values, the maximum traffic flow capacity can be calculated by multiplying the width and the maximum traffic flow capacity per unit width (i.e., 1.3 persons/m/s and 5 cars/m/s for pedestrians and cars, respectively). Finally, the storage capacity of the link representing the capacity of the link in agent/m^2, i.e., is calculated as the product of the areas (m^2) and the maximum density per unit area (pedestrians/m^2 or cars/m^2) [12].

Furthermore, the agents' plans are generated using the location/coordinates, departure time, and final destinations. In this study, the total agents are ~ 2,200 generated from the nine sub-districts of Saga, including Myojin, Kaisho, Hamamachi, Yokohama, Owada, Shimobun, Machibun, Umaji, and Sakori (Fig. 4b). The departure time is set to 10:00 a.m. as the evacuation simulation is assumed to occur in the daytime, and the final destination of the agents is the evacuation points (Fig. 4a). Such a departure time is chosen to evaluate the evacuation at the most crowded daily scenario since commuters come to Saga district (~500 people) during the daytime for weekday work. The agents are also assumed to evacuate simultaneously by defining the same initial reaction time, 5 min, because local residents are familiar with the evacuation during a disaster due to regular evacuation drilling in the study areas. The agent departure location is defined as the following: 600 people in houses and 1,600 people at schools, factories, markets, and non-residential buildings. Most people are outside their houses because it is working hours and school time. Moreover, 600 people inside the houses comprise 70 % of the older people above 65. In addition, the capacity of evacuation points depends on the transportation modes. For the pedestrian model, the evacuation capacity is set to be infinite because those points can only be accessed by foot and have sufficient capacity to accommodate the local residents of Saga. However, for the car model, the capacity needs to be limited as those evac-

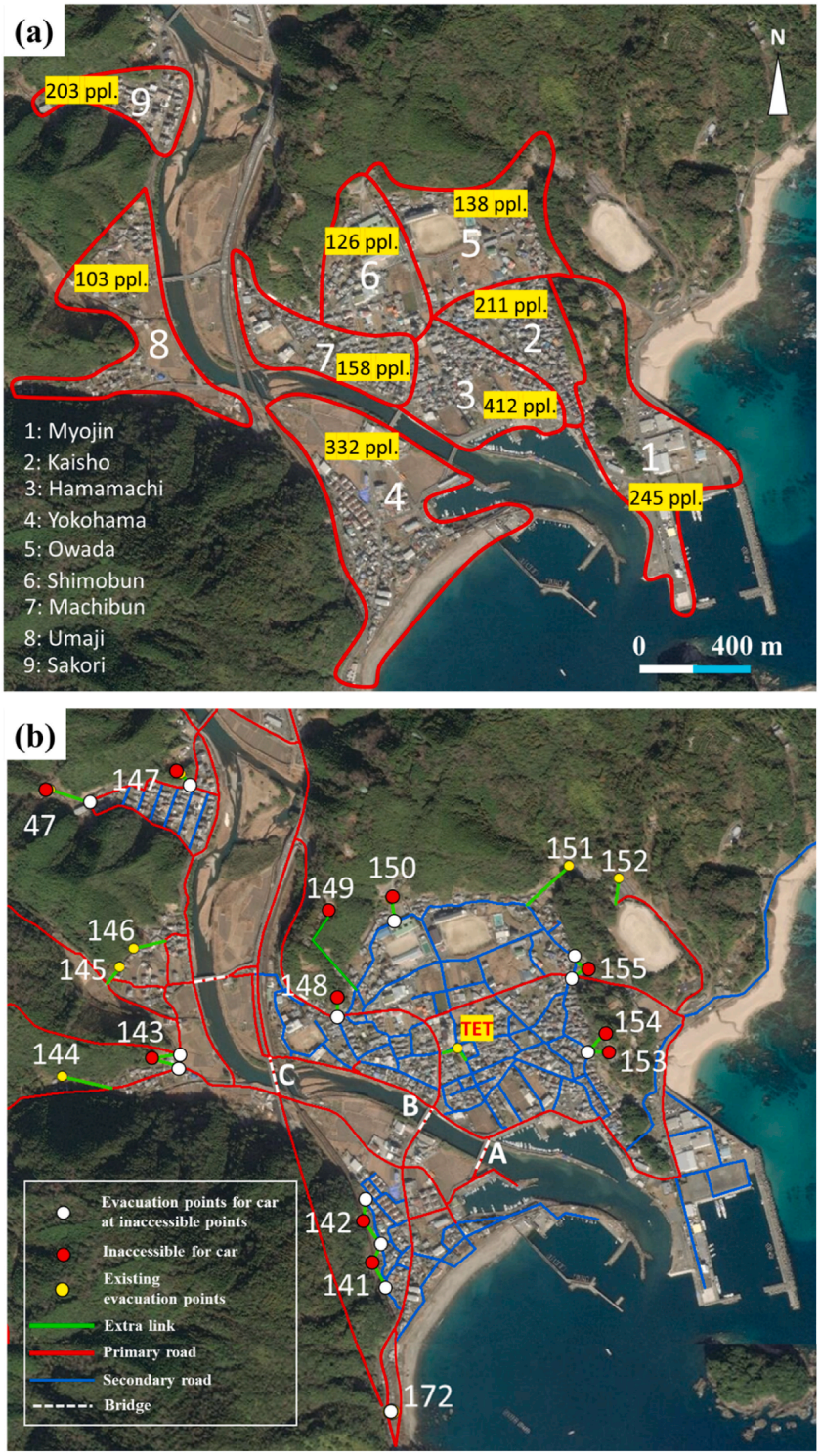

Fig. 4. Considered areas for evacuation simulation (a) and network data in the Saga district (b).

uation points cannot be accessed by cars. Hence, the capacity varies from 10 to 100 cars, depending on the parking capacity (more details are provided in [17].

Simulations are carried out using different scenarios based on the transportation mode used by the agents to the evacuation points. Therefore, four types of transportation modes are introduced in this study, including (1) single pedestrian model, (2) single car model, and two models of multimodal combining the pedestrian and car, i.e., (3) 90 % pedestrian – 10 % car (Multimodal – 1: MM1) and (4)

75 % pedestrian – 25 % car (Multimodal – 1: MM2). Such a setup is used because most of the population in Saga will evacuate on foot, as the distance from home/office to evacuation points is relatively short. The transportation mode in the MATSim simulation is distinguished by the speed, and hence, the speeds of 1 m/s – 2 m/s and 8.3 m/s are used to represent pedestrians and cars, respectively [35–38]. Those speeds are uniformly distributed depending on the considered scenarios. The agent-based tsunami evacuation modelling is finally performed using MATSim based on the input data above.

2.4. Tsunami casualty risk assessment

The casualty risk assessment in this study is evaluated using the number of affected people, i.e., those who do not have enough time to evacuate and are trapped by the tsunami wave. Such a parameter is calculated by comparing the results of the stochastic tsunami simulation (i.e., tsunami arrival times at links) and the agent-based evacuation modelling (i.e., tsunami evacuation times at links). The level of tsunami depth considered to affect the agent during the evacuation is 0.3 m [39,40]. Therefore, the tsunami arrival times involving the number of affected people estimation are defined when the tsunami depth reaches 0.3 m.

A generic agent j is considered entrapped by a tsunami at the node i of the evacuation path K_j if the wave arrival time at the same node (T_i) is lower than the agent's arrival time (t_{ij}) [12]. During the overall evacuation journey and for the entire transportation system, a generic evacuee agent j is considered affected if the minimum of the differences between T_i and (t_{ij}) for all the nodes along the evacuation path K_j of the agent j is lower than zero:

$$\min_{\forall\, i \in K_j} \left[T_i - t_{ij}\right] < 0 \tag{2}$$

The number of affected people is calculated for each source model from the two magnitude cases (i.e. M8.8 and M9.0). Subsequently, the number of affected people estimation may become a stable risk metric for developing a robust decision variable for effective tsunami evacuation maps in coastal regions.

3. Results and discussion

In this section, the stochastic tsunami hazard assessment results in terms of tsunami hazard level and tsunami evacuation time are first presented. A total of 1,000 tsunami hazard data from the 1,000 stochastic source models generated from the M 8.8 and M 9.0 scenarios are presented. Second, the tsunami casualty risk estimation using agent-based evacuation modelling from different mode scenarios is shown, followed by an assessment of the impact of the TET in Saga (Fig. 2d) on the mitigation plan. Finally, a recommendation for mitigation strategies in tsunami-prone regions is drawn based on the integration of tsunami risk assessment of stochastic tsunami hazard, exposure, risk, and agent-based evacuation modelling.

3.1. Stochastic tsunami hazard assessment

This section presents a tsunami hazard assessment in Saga in terms of inundation depth maps, tsunami depth, and tsunami arrival times. The tsunami inundation maps evaluate the effectiveness of assigned evacuation points, whereas the tsunami depth and arrival time show the risk during the evacuation process. Fig. 5 shows the maximum inundation depth maps for the 50th and 90th percentiles of the 500 stochastic hazards from each magnitude scenario (i.e. M8.8 and M9.0). These two percentiles represent the critical tsunami hazard zones in the Saga district. Moreover, the locations of tsunami evacuation points are also plotted along with the inundation zone to highlight the effectiveness of tsunami evacuation points assigned by the local government.

Fig. 5 confirms that significant tsunami hazards reaching more than 15 m depth can inundate coastal areas of the Saga district (Fig. 5). Moreover, the existence of the Iyoki River connected to the sea may lead to a significant tsunami hazard in the Saga district. The worst scenarios (i.e., 90th percentile) for both cases, i.e., M8.8 and M9.0, show that considerable tsunami depths can occur in the centre of the town due to the flow of tsunami waves from the Iyoki River (>10 m). In general, the assigned tsunami evacuation points by the local government are located in safe positions. All 17 horizontal tsunami evacuation points (i.e., evacuation to higher grounds) are situated in non-inundated areas, meaning that the local government developed a well-prepared plan for the evacuation. Moreover, the locations of evacuation points in high-density population areas (the dash-circle in Fig. 5d) are highly essential to save people's lives because significant tsunami hazard may occur in those areas. In particular, the TET can be used as a temporary tsunami shelter for those who cannot go further north to reach the higher-ground evacuation points (Fig. 5). The inundation map from the worst-case scenario (i.e., the 90th percentile of the M9.0 case) also confirms that the height of the TET is also sufficient (> 20 m) to be entirely functional during the tsunami (Fig. 5d).

The maximum tsunami depth is evaluated for fifteen points along the coast of Saga (Figure 6a). The stochastic tsunami simulation model has successfully captured the uncertainty of tsunami depth, displaying the variability of maximum tsunami depths along the coast (Figure 6b and c). The results clearly show that the maximum tsunami depth is significantly high for both magnitude scenarios (i.e., M8.8 and M9.0), reaching more than 20 m (Fig. 6b and c). Such a value may produce extensive social and economic losses. Furthermore, tsunami arrival times of 0.3 m deep water at the 15 points are presented (Fig. 6d and e). The tsunami arrival time ranges between 5 and more than 60 min. The majority of the simulation results are centred around 20–30 min. In general, the results highlight that the assigned tsunami evacuation points are incredibly important to save the local population as the tsunami may arrive very quickly (i.e., 5 min). Therefore, the community reaction time for this region needs to be at most 5 min so the people can evacuate from the coastal areas safely.

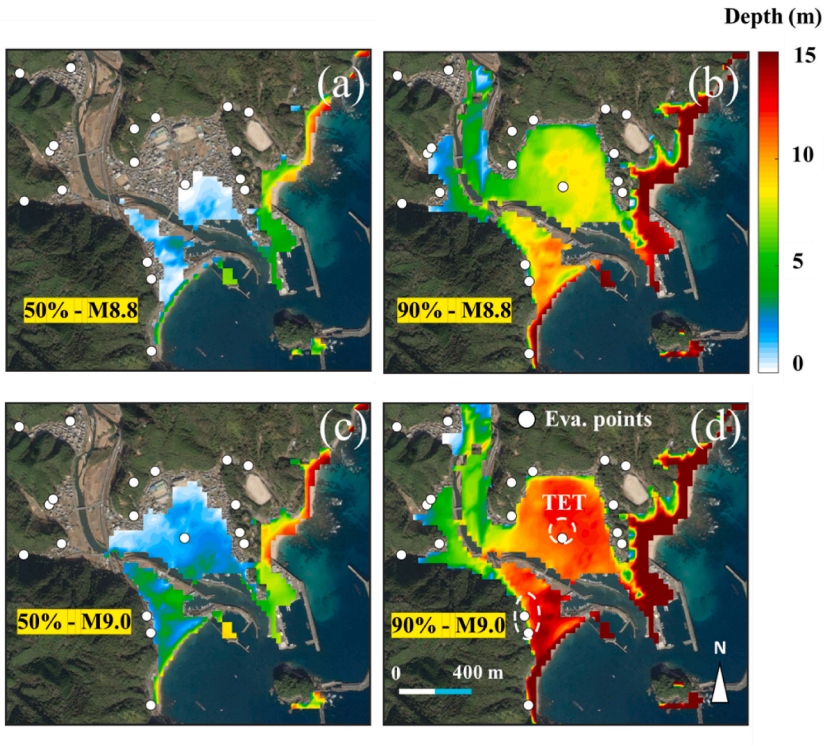

Fig. 5. Tsunami inundation maps of M 8.8 (a and b) and M 9.0 (c–d) case taking at the 50th and the 90th percentiles.

3.2. Tsunami evacuation time and casualty risk assessment

To evaluate the impact of using different transportation modes during the evacuation, the agents' evacuation time in the form of spatial plots and histograms produced from the four models are presented in Fig. 7. Statistical data of agents' evacuation times, including mean and standard deviation, are also shown in the figure.

The pedestrian model performs the best compared to the other transportation modes, showing the quickest evacuation time with an average of 9.7 min (Fig. 7a and b). The spatial plot from the pedestrian model also highlights that the agents have sufficient time to evacuate to the safe areas. Most of the agents have evacuation times between 5 and 15 min. The evacuation times from the multimodal models are also almost identical with slight evacuation time differences of mean and standard deviation, i.e. 10.4 vs 10.7 min and 4.2 and 4.7 min, respectively (Fig. 7e–h). In addition, the multimodal model produces only 1 min slower evacuation time compared to the pedestrian model because of sufficient evacuation capacity for 600 car users (25 % of the total agents). On the other hand, the car model performs the worst among the three transportation modes. About 300 agents are found to have more than 25 min of evacuation time and are highlighted with the red dots distributed around the coast and the densely populated areas (Fig. 7c). The average evacuation time for the car model is also ~ 4 min slower than the pedestrian model (Fig. 7d vs Fig. 7b). Notably, the evacuation time produced from the MATSim simulation is an optimized scenario where the plan is executed ideally. Such an approach may suit a well-prepared country against disasters like Japan, as evacuation drilling is carried out regularly. Therefore, when the MATSim simulation is implemented in other regions, some adjustments in the simulation setup need to be adopted, e.g., longer initial reaction time or undefined evacuation plans because of no regular drilling. Moreover, the daytime evacuation may also influence the evacuation duration. Nighttime evacuation may take longer due to the difficulty in accessing the network and the longer initial reaction [14].

Subsequently, the number of affected people is calculated by integrating the tsunami arrival times from the 500 stochastic models for each magnitude case (i.e., a total of 1,000 models) and the times during evacuation. The probability of the number of affected people generated from different transportation modes is further presented in Fig. 8. From the perspective of casualty risk assessment, the car model may also lead to significant risk due to the arrival of the tsunami in the Saga district. The results from both magnitude cases indicate that at least ~ 200 people may be trapped by the tsunami during their evacuation process, with a maximum affected people number of about 1,000 people (see black lines in Fig. 8a and b). Moreover, about 40 % probability of having 500 to 1,000 people affected by the tsunami is found for both magnitude cases when the car is used as a transportation mode to the evacuation points. Such a number is significantly different in comparison to the other three modes. The comparison at a 35 % probability level at an M9.0 magnitude case shows that the tsunami will affect about 10 and 100 people for the pedestrian and the two multimodal models, respectively. The number increases three times more than the pedestrian model when the car model is considered, i.e., reaching ~ 1,000 people. Generally, the pedestrian model performs the best with the lowest number of affected people, followed by the MM1 and MM2, respectively. Both multimodal models also produce similar results with the pedestrian model with a maximum affected people num-

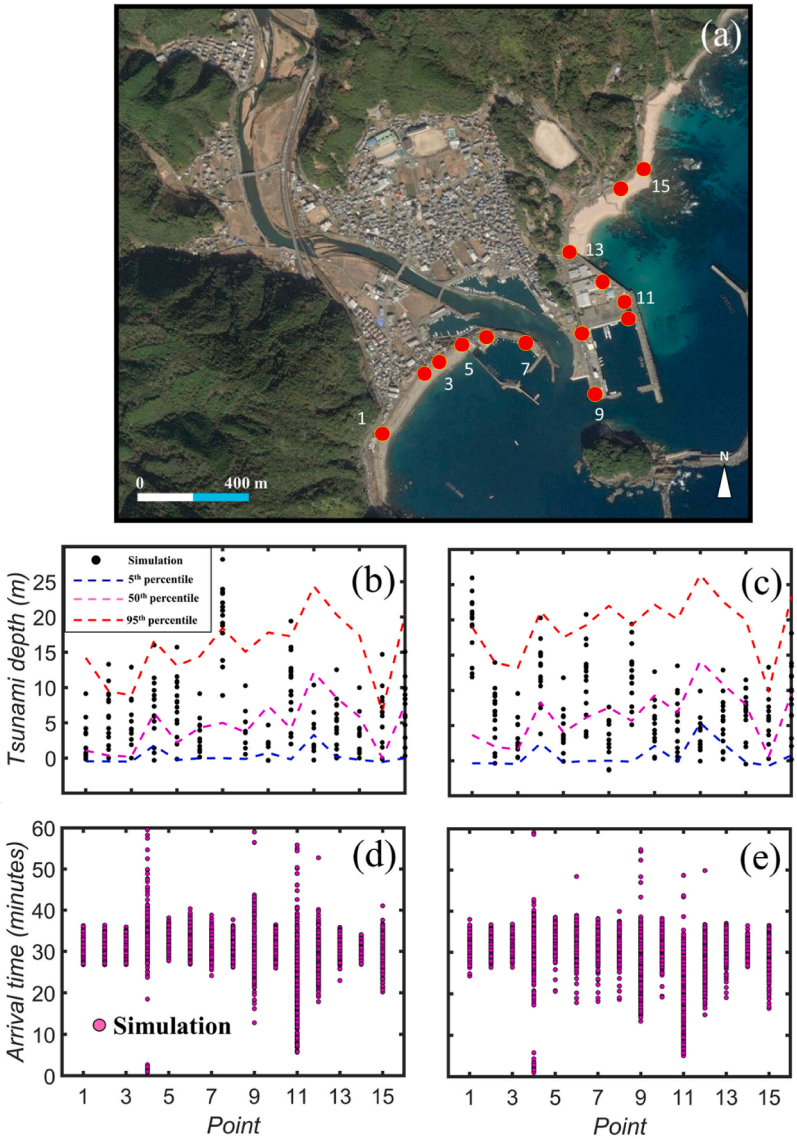

Fig. 6. Maximum tsunami depth (b–c) and arrival times (d–e) along the coast of the Saga district for the magnitude of M8.8 (b and d) and M9.0 (c and e).

ber of ~ 200 people. In addition, these results suggest that it is highly recommended not to use a car during the evacuation when the tsunami warning is issued. The capacity of evacuation in the car model is limited by space and total road areas close to the evacuation points (see [17] for details). Therefore, the use of cars may result in congestion and queuing during evacuation. Most of the population should evacuate by foot. Car evacuation may be an option, but it is not recommended to be used in the first place. Otherwise, a significant risk may occur during the evacuation once the number of cars used by the local people is high (> 25 % of the total population).

3.3. Impact of tsunami evacuation tower on risk reduction

The existing TET is extremely useful in tsunami-prone areas to reduce fatalities. Hence, this section aims to evaluate the effectiveness of TET in fatality risk reduction. The cases from four different transportation modes with PassingQ are presented in simulated scores, evacuation times, and affected people to assess the impact of TET on saving people's lives. Three types of scores are considered in this evaluation, including the average best score (red line), average score (blue line), and average worst score (black line).

Fig. 9 presents the simulated scores from eight models of both with (right panel) and without (non-TET; left panel) TET generated from four different modes: pedestrian (Fig. 9a and b), car (Fig. 9c and d), MM1 (Fig. 9e and f), and MM2 (Fig. 9g and h). The TET does not influence the pedestrian model scores, as both show constant scores at the level of 115 (this result is because the size of the pedestrian agent, compared to the width of the infrastructure, is such that it is impossible to have congestion). The change can be seen clearly for the car model, where the worst average score for the TET model is lower than the non-TET model, resulting in lower

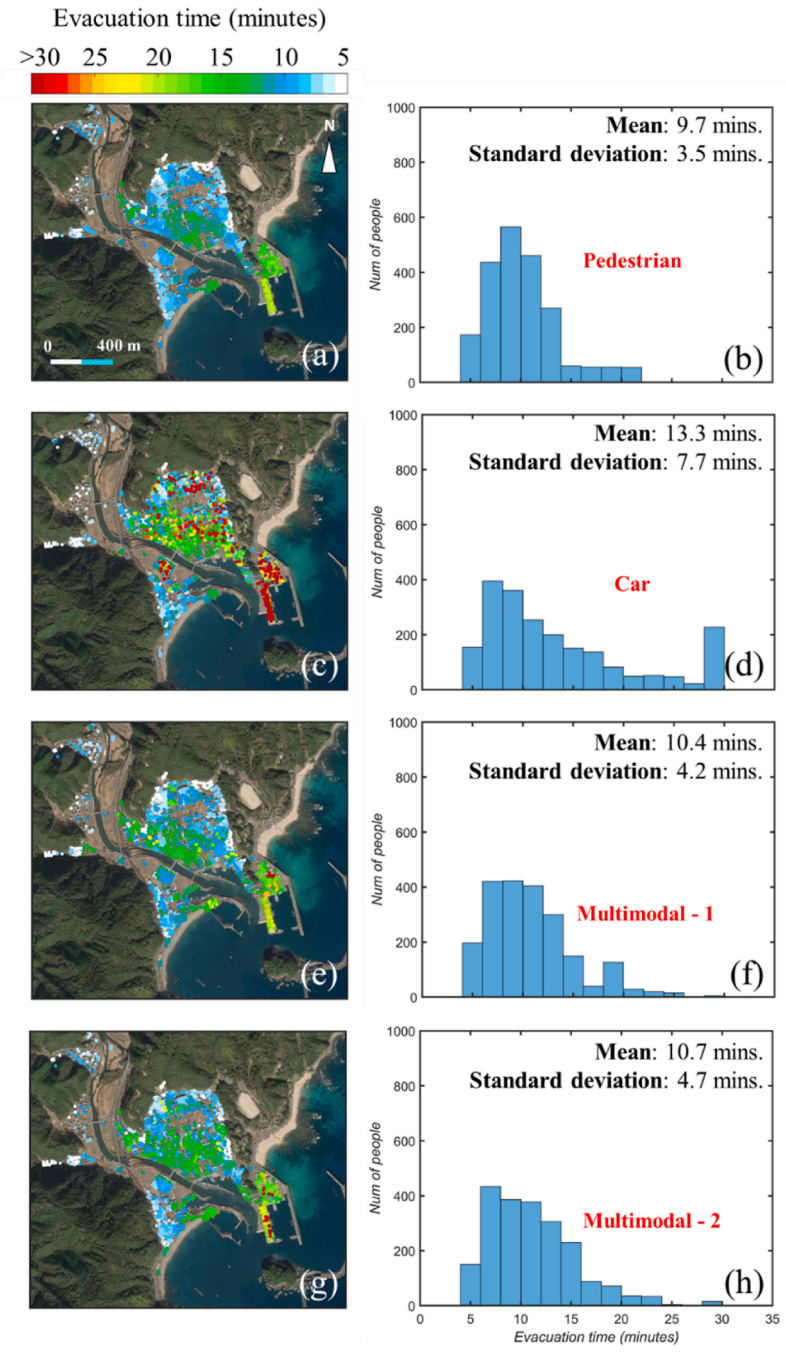

Fig. 7. Spatial plot (left panel) and histogram (right panel) of agents' evacuation time from the pedestrian (a and b), car (c and d), multimodal – 1, MM1 (e and f) and multimodal – 2, MM2 (g and h) models.

average scores. Such a trend is due to the limitation of the link's capacity surrounding the TET areas where congestion can occur. However, the existing TET may add an extra evacuation option for the agents. Hence, the evacuation route may be shorter with the TET for the agents near the TET. Consequently, the uncertainty of scores for the TET model is less than the non-TET model; it ranges from −10 to 10 and 0 to 50 for the TET and non-TET models, respectively. Because of a small percentage of the car (i.e., 10 %), the impact of the TET is also insignificant for the MM1 case. The scores of MM1 for both TET models range from 90 to 110. The score differences are more noticeable when the MM2 is considered, where the worst average score for the TET model is slightly lower than the non-TET model. In general, the existing horizontal evacuation points to the higher ground are sufficient to accommodate the local residents in Saga. Hence, the existence of TET does not significantly impact the overall simulated scores involving all agents, particularly for the non-car model.

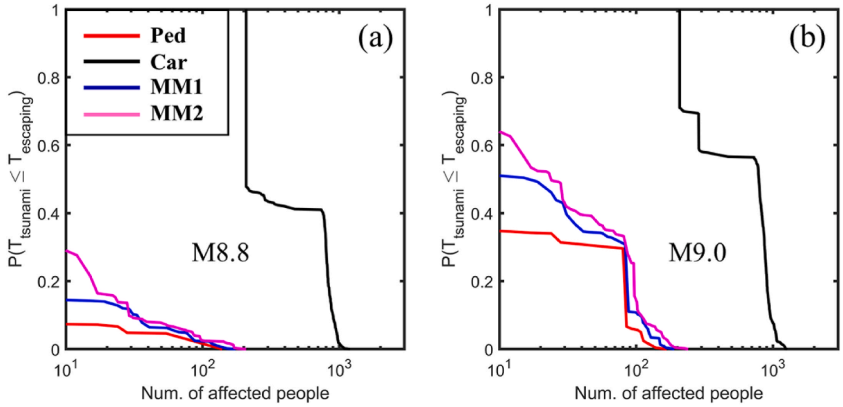

Fig. 8. Probability of the number of affected people from different transportation modes for the case of M8.8 (a) and M9.0 (b).

The spatial plots and histograms of evacuation times, along with the mean and standard deviation, are presented in Fig. 10 to evaluate the performance with and without the TET models. Generally, TET's existence significantly reduces the evacuation time of agents close to the TET. The results of the TET model from all types of transportation modes demonstrate the change in tsunami evacuation time at the central Saga, where the TET is located. For instance, the agents' evacuation time located near the TET for the pedestrian model decreases from 15 min to 5 min owing to the existence of TET (Fig. 10a and c). The drastic change may also be seen for the car model when almost no agents have more than 30 min evacuation times for the TET model compared to the non-TET model (i.e., ~ 100 agents have evacuation times of >30 min; Fig. 10e–h). In addition, the multimodal models show a similar trend with quicker evacuation times of the agents located near the TET (i.e. 15 and 5 min of agents' evacuation times located near the TET for the non-TET and TET models, respectively; Fig. 10i-o). However, the overall trend shows that the TET only affects the agents' movements close to the TET, and the other agents still have access to the higher ground evacuation points. Subsequently, the average and standard deviation of evacuation time of the agents from the non-TET model are only ~ 1 min slower than the TET model. This also emphasizes that the current evacuation points at high grounds are effective as they can sufficiently accommodate the residents of the Saga district during the tsunami event.

The probability of the number of affected people in all models is further calculated and presented in Fig. 11. The change in terms of the probability of the affected population is insignificant for all models. However, in general, for the TET model the probability is slightly smaller with respect to the non-TET model. Such a small change is because of the following reasons. First, the TET only significantly shortens the agents' evacuation times near the tower; hence, the impact on overall agents is insignificant. Second, the most critical agents are located close to the coastal line and the river, whilst the TET is located near the centre of Saga, relatively far from the coast. Subsequently, the critical agents trying to access the TET may already be affected by the tsunami during the evacuation, leading to a slight change in the number of affected people. Moreover, the numbers of affected people for the car model in both TET and non-TET models and the two magnitude cases (M8.8 and M9.0) are still significant (>200 people). Therefore, it is not highly recommended to use the car as a means of evacuation (Fig. 11). On the other hand, the other transportation modes show a relatively small number (maximum of 100 people) of affected people compared to the car model, even with the existing TET. However, there is a significantly different number of affected people for the MM2 model between the non-TET and TET models for the case of M9.0 at the 40 % probability level, i.e., 15 agents are affected for the TET models in comparison to the 40 affected agents in the non-TET models (56 % difference).

To clearly see the impact of TET on the evacuation, the spatial plots of affected agents due to the tsunamigenic event of M9.0 are displayed. Figs. 12 and 13 show the median and the 90th percentile of the affected people generated from the 500 M9.0 stochastic models. The 90th percentile may represent the worst-case scenario during the evacuation. The red dot represents the affected people, with their total number written in each figure, while the white dot shows the non-affected people. The trend of affected people may not be obviously seen at the median level as the number of affected people for all cases except for the car model is zero. These results show that at the median level, the Saga residents are generally not affected by the tsunami unless the majority evacuate to the evacuation points using a car. Moreover, higher-ground evacuation points are sufficient to accommodate all residents as the non-TET model for the median case from the three models (i.e., pedestrian, MM1, and MM2) shows zero affected people (Fig. 12a and b and Fig. 12e–h). In contrast, the distribution of affected people may be noticeable for the worst-case scenario (i.e., the 90th percentile case), as shown in Fig. 13. The figure indicates that the critical agents are close to the coastal line and the Iyoki river. For the pedestrian and the two multimodal models, the agents located in the harbour and markets near the coast are majorly affected by the tsunami, with the number of affected people reaching 140 people (Fig. 13a and b and Fig. 13e–h). Those who work in the fish company and the market on the southeast coast of the Saga district may also be severely affected by the tsunami. In all cases, some affected agents are located in those areas, particularly in the car model case. More importantly, the impact of the TET may be detected through these spatial plots. In general, the affected agents can still be shown at the centre of Saga, where the TET is located, particularly for the non-TET model. The existence of the TET saves those people, and the number of affected people near the TET is finally reduced.

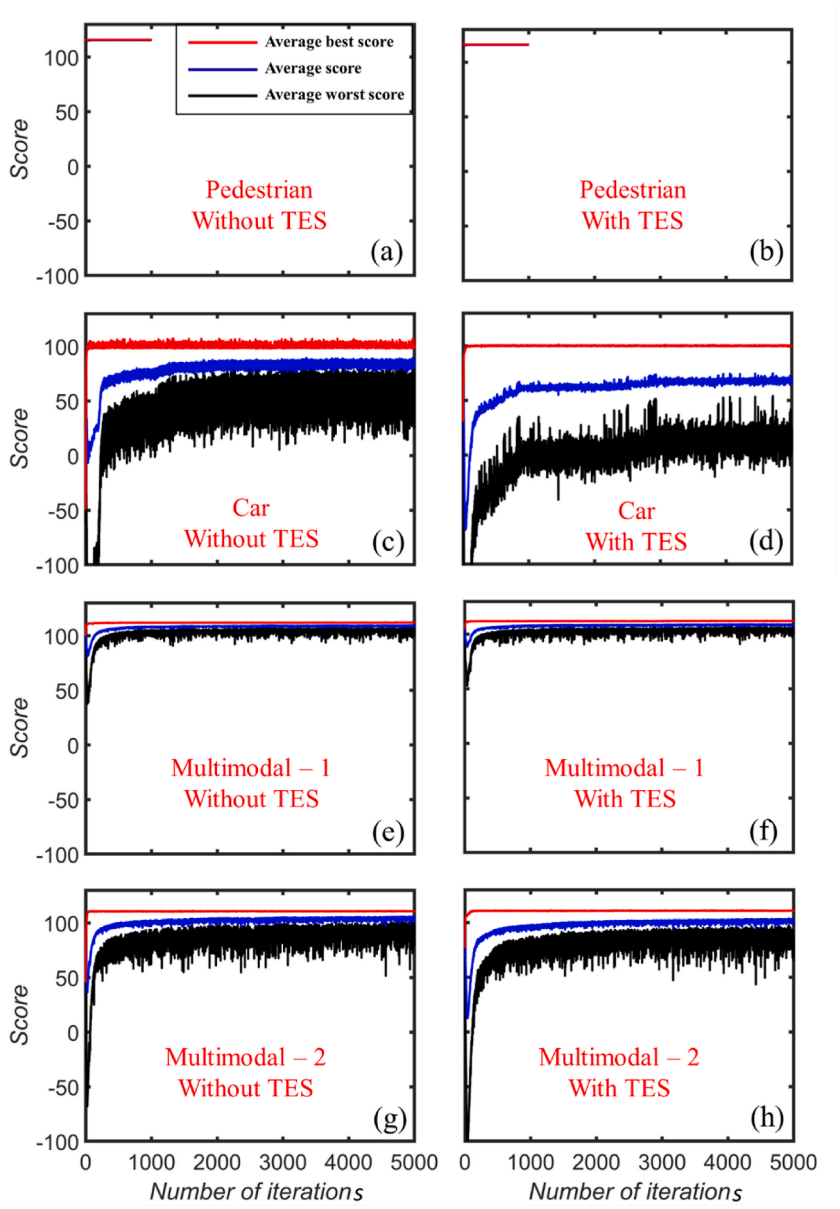

Fig. 9. Scores produced from the model of with (left panel) and without (right panel) TET for the case of pedestrian (a and b), car (c and d), multimodal – 1 (e and f) and multimodal – 2 (g and h) models.

4. Recommendation of mitigation strategies

An extensive study integrating stochastic tsunami hazard, exposure, risk, and agent-based evacuation modelling has been carried out in the Saga district, Kuroshio, Japan. In addition, detailed investigations on agent-based evacuation modelling using MATSim, including evaluating the iteration number of simulation, the evacuation modes, the dynamic of the links, and the existing tsunami evacuation points, have also been done. The results from these investigations may subsequently be used to recommend the following mitigation strategies learned from the Japanese experience.

First, the evacuation points on the higher grounds need to be assigned by the local government of the tsunami-prone regions. The evacuation option to the higher ground has to be distributed near high-density populated areas. The evaluation of designated higher-ground evacuation points in the Saga district has indicated that those points successfully reduce evacuation times and save people's lives (Fig. 10). Second, those higher ground evacuation points are recommended to be placed at larger flat areas to accommodate a significant number of people (hundreds of people). All of the evacuation points in the Saga district have these two features: (1) located on higher grounds (>20 m) and (2) have large areas of evacuation (i.e., can accommodate hundreds of people; Fig. 4b). Third, evacuation points need to be easily accessible and connected to the main road networks. Moreover, clear signs at those evacuation points along the network may need to be appropriately installed to lead the people to safe areas and reduce congestion during the

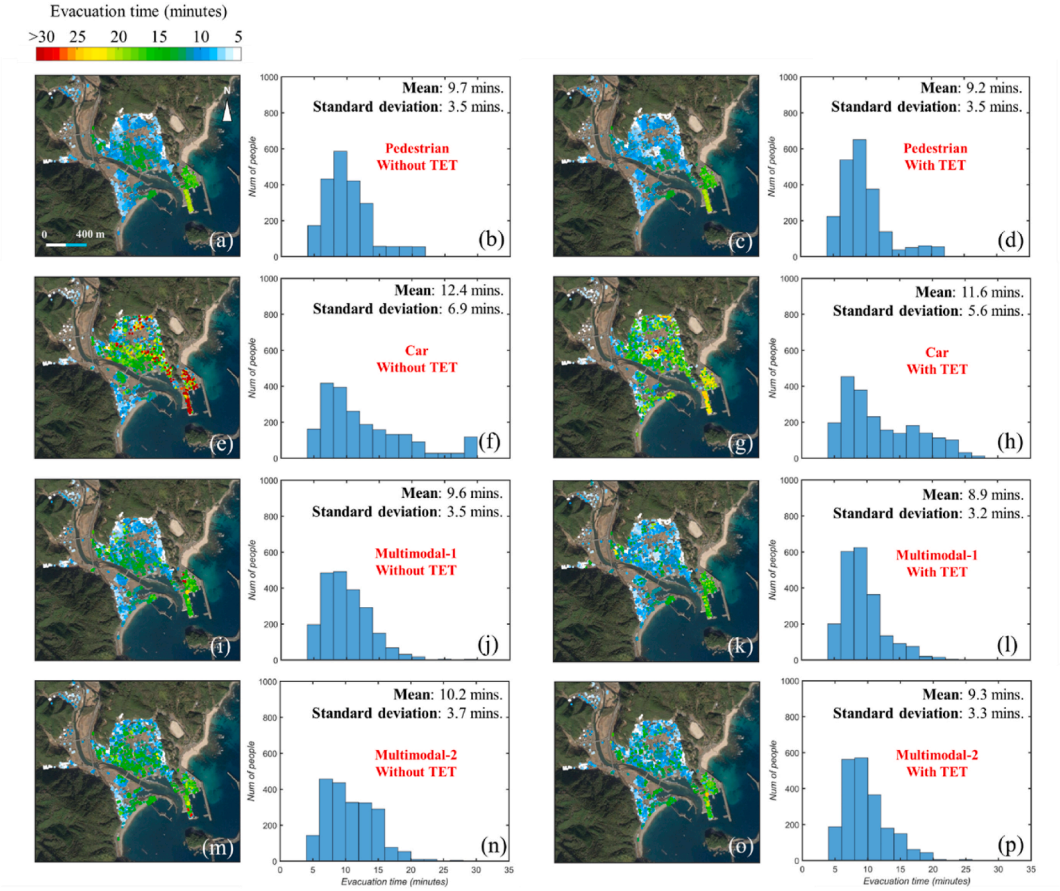

Fig. 10. Spatial plot and histogram of agents' evacuation time for the model with (left panel) and without (right panel) TET from the pedestrian (a to d), car (e to h), multimodal – 1 (i to l) and multimodal – 2 (m to p) models.

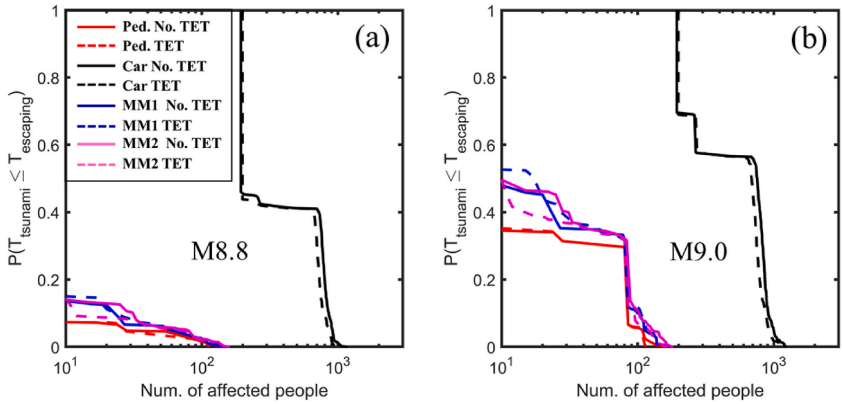

Fig. 11. Probability of the number of affected people from the TET and non-TET models for the case of M8.8 (a) and M9.0 (b).

evacuation. Fourth, the tsunami evacuation tower is highly recommended to be built appropriately and placed in densely populated areas where congestion is expected to occur during the evacuation. The location of the TET in Saga is an excellent example of locating the tsunami evacuation tower, which is placed near the centre of Saga district with densely populated areas (Fig. 1b and c). Fifth, it is highly recommended to evacuate on foot. Evacuating using a car or motorbike may lead to congestion and increase the risk of getting affected by the tsunami [17]. The case in Saga has also demonstrated such a recommendation as the car evacuation model produces a longer evacuation time and the highest number of affected people by the tsunami (>1,000 people; Figs. 7 and 13). Sixth, the population most at risk is located near the coast and the river, and hence, a possible tsunami shelter with sufficient height (>15 m) may need to be assigned close to those areas. Such a shelter may be used as an emergency evacuation shelter as the people may get hit by

Fig. 12. Spatial plot of affected people generated from the median of the 500 M8.8 stochastic cases.

the tsunami during the evacuation to the far evacuation points. Finally, the evacuation route needs to avoid the network near the coast and the river.

In addition, the proposed framework can generally be adopted for tsunami risk assessment in other tsunami-prone countries. However, several aspects need to be updated to consider the regional features of the applied regions. First, the level of evacuation readiness in terms of evacuation points availability and the drilling frequency may define the evacuation setup in agent-based modelling. The availability of evacuation points may determine the final destination of the evacuee, whilst the evacuation drill frequency may be used to set up the evacuation route. The evacuation points must be pre-defined before the simulation with various assumptions and simplifications when the study areas do not have the proposed evacuation point. Moreover, the study area with low evacuation drill frequency may not use the shortest evacuation route to the safe points as the agents may use different routes with respect to the shortest path. Second, the type of transportation mode needs to consider the typical local transportation mode, e.g. in Indonesia it is better

Fig. 13. Spatial plot of affected people generated from the 90th percentile of the 500 M9.0 stochastic cases.

to use pedestrians and motorbikes for evacuation than on foot and cars like in Japan [17]. Third, the variation of departure time can be used to evaluate more evacuation cases to define the most vulnerable period for evacuation.

5. Conclusions and limitations

This research presented for the first time an integration of stochastic tsunami hazard, exposure assessment, and agent-based evacuation modelling to develop a comprehensive framework for tsunami casualty risk assessment aimed at risk management and decision-making. Such a framework was applied to the Saga district of Kuroshio, Japan. The case study was deemed of interest following past investigations on the tsunami hazard [21,22], tsunami risk [3,8,23]; [19] [7,9], and tsunami evacuation [17]. Such initial studies were convoluted for the first time in a multi-disciplinary way to obtain a rational, integrated framework.

First, the stochastic earthquake source models for the magnitude values of M8.8 and M9.0 were simulated for the Nankai-Tonankai thrust and further adopted as a starting point for the tsunami propagation and inundation. Second, the results in terms of

stochastic tsunami hazards were prepared and processed at each link and node of the transportation network to carry out the risk assessments later. Third, a comprehensive agent-based tsunami evacuation modelling using MATSim was performed. A sensitivity analysis was also conducted on the simulation parameters, including the number of iterations, transportation modes (e.g., pedestrians only, pedestrians, and cars), and the dynamics of the link (i.e., queue management). The impact of a tsunami evacuation shelter as a mitigation strategy was also implemented in some evacuation scenarios and assessed for efficiency. Recommendations on tsunami mitigation strategies were finally defined based on the framework results.

A significant tsunami hazard was anticipated for the case of M9.0 in the Saga district, with a tsunami depth of 10 m and 15 m along the coast and the Iyoki River, respectively. The tsunami arrival time ranged between 5 and 30 min. In this study, the worst-case tsunami inundation map (i.e., 90th percentile for the M9.0 scenario) was further used to evaluate the 17 evacuation points defined by the local government. It showed that those evacuation points are well placed as they are located outside the inundation areas. Furthermore, the existing TET, being taller than 20 m, was also judged effective as it stands above the expected tsunami depth level (maximum of 15 m). Therefore, the TET can effectively accommodate the residents at the centre of Saga, which is the district's most densely populated area.

Regarding evacuation suggestions, the local population in Saga is highly recommended to evacuate on foot and not to use the car as a means of transportation during the evacuation. Using the car may cause congestion, leading to a higher number of affected agents (i.e., in the case of Saga, the number of affected agents can be more than 1,000 people). Some people may use cars to access the evacuation points, but it is recommended that no more than 25 % of the population use the car to reduce risk during the evacuation. Finally, it was found that the existence of a TET has a significant impact on the population located closer to the TET. However, it had an insignificant effect globally because of the sufficient number of higher-ground evacuation areas.

Moreover, some limitations of this research are the following. First, the optimized MATSim simulation procedure setup in this study may result in an ideal situation suitable for a well-prepared disaster country (e.g. Japan); therefore, adjustments in the setup of MATSim simulation are needed for other regions. Second, the departure time is the same for all agents. Future studies need to address the different behaviour of each agent in reacting to evacuation; hence, the departure time should be defined as variable per agent (e.g., age-dependent). Third, only the daytime scenario is investigated in this study. Variations in departure time (i.e., daytime vs night) may need to be considered for future studies. Finally, our agent-based evacuation modelling results have not been validated using real drilling or past tsunami evacuation data. Future studies will need to validate such an agent-based evacuation modelling against data if available.

Credit author statement

Katsuichiro Goda: Conceptualization, Data curation, Funding acquisition, Methodology, Resources, Validation, Writing – review & editing. Nobuhito Mori: Conceptualization, Data curation, Methodology, Validation, Writing – review & editing. Tomohiro Yasuda: Conceptualization, Validation, Writing – review & editing, Data curation, Methodology. Flavia De Luca: Conceptualization, Methodology, Project administration, Supervision, Visualization, Writing – review & editing, Resources. Widjo Kongko: Writing – review & editing, Validation. Ario Muhammad: Conceptualization, Data curation, Methodology, Software, Visualization, Writing – original draft. Raffaele De Risi: Conceptualization, Data curation, Formal analysis, Methodology, Supervision, Visualization, Writing – review & editing.

Declaration of competing interest

The authors declare the following financial interests/personal relationships which may be considered as potential competing interests: Flavia De Luca reports financial support was provided by Leverhulme Trust. Ario Muhammad reports financial support was provided by Bristish Council. Raffaele De Risi reports financial support was provided by European Cooperation in Science and Technology.

Data availability

Data will be made available on request.

Acknowledgements

This work was supported by a Researcher Links Climate Challenge Workshop Grant, ID 714949392 and funded by the British Council to implement activities in the run-up to COP26 (the 26th United Nations Climate Change Conference of the Parties). For further information, please visithttps://www.britishcouncil.org/sites/default/files/27012021_rlcc_-_announcement_2.pdf. Moreover, this research is also funded by the Leverhulme Trust (RPG-2017-006, GENESIS project). All authors contributed to this work, playing different roles. RDR acknowledges the COST Action CA18109 AGITHAR, supported by COST (European Cooperation in Science and Technology). The authors are grateful for the contribution received by the three anonymous reviewers whose comments have significantly improved the quality of the paper.

References

[1] United States Geological Survey (Usgs), Latest Earthquakes, 2015. http://earthquake.usgs.gov/earthquakes/map/.
[2] T. Takabatake, M. Esteban, I. Nistor, T. Shibayama, S. Nishizaki, Effectiveness of hard and soft tsunami countermeasures on loss of life under different population scenarios, Int. J. Disaster Risk Reduc. 45 (2020) 101491.

[3] A. Muhammad, K. Goda, N. Alexander, Tsunami hazard analysis of future megathrust sumatra earthquakes in Padang, Indonesia using stochastic tsunami simulation, Frontiers in Built Environment 2 (2016) 33.
[4] A. Grezio, A. Babeyko, M.A. Baptista, J. Behrens, A. Costa, G. Davies, H.K. Thio, Probabilistic tsunami hazard analysis: multiple sources and global applications, Rev. Geophys. 55 (4) (2017) 1158–1198.
[5] J.D. Griffin, I.R. Pranantyo, W. Kongko, A. Haunan, R. Robiana, V. Miller, H. Latief, Assessing tsunami hazard using heterogeneous slip models in the Mentawai Islands, Indonesia, Geological Society, London, Special Publications 441 (1) (2017) 47–70.
[6] J. Behrens, F. Løvholt, F. Jalayer, S. Lorito, M.A. Salgado-Gálvez, M. Sørensen, E. Vyhmeister, Probabilistic tsunami hazard and risk analysis: a review of research gaps, Front. Earth Sci. 9 (2021) 114.
[7] K. Goda, T. Yasuda, N. Mori, A. Muhammad, R. De Risi, F. De Luca, Uncertainty quantification of tsunami inundation in Kuroshio, Kochi Prefecture, Japan, using the Nankai–Tonankai megathrust rupture scenarios, Nat. Hazards Earth Syst. Sci. 20 (11) (2020) 3039–3056.
[8] A. Muhammad, K. Goda, N.A. Alexander, W. Kongko, A. Muhari, Tsunami evacuation plans for future megathrust earthquakes in Padang, Indonesia, considering probabilistic earthquake scenarios, Nat. Hazards Earth Syst. Sci. 17 (12) (2017) 2245.
[9] K. Goda, R. De Risi, F. De Luca, A. Muhammad, T. Yasuda, N. Mori, Multi-hazard earthquake-tsunami loss estimation of Kuroshio Town, Kochi Prefecture, Japan considering the Nankai-Tonankai megathrust rupture scenarios, Int. J. Disaster Risk Reduc. 54 (2021) 102050.
[10] N. Zarboutis, N. Marmaras, Design of formative evacuation plans using agent-based simulation, Saf. Sci. 45 (9) (2007) 920–940.
[11] X. Chen, F.B. Zhan, Agent-based modelling and simulation of urban evacuation: relative effectiveness of simultaneous and staged evacuation strategies, J. Oper. Res. Soc. 59 (1) (2008) 25–33.
[12] G. Lämmel, M. Rieser, K. Nagel, H. Taubenböck, G. Strunz, N. Goseberg, J. Birkmann, Emergency preparedness in the case of a tsunami—evacuation analysis and traffic optimization for the Indonesian city of Padang, in: Pedestrian and Evacuation Dynamics 2008, Springer, Berlin, Heidelberg, 2010, pp. 171–182.
[13] J. Kim, S. Lee, S. Lee, An evacuation route choice model based on multi-agent simulation in order to prepare Tsunami disasters, Transport. Bus.: transport dynamics 5 (4) (2017) 385–401.
[14] N. Wood, K. Henry, J. Peters, Influence of demand and capacity in transportation simulations of short-notice, distant-tsunami evacuations, Transp. Res. Interdiscip. Perspect. 7 (2020) 100211.
[15] H. Wang, A. Mostafizi, L.A. Cramer, D. Cox, H. Park, An agent-based model of a multimodal near-field tsunami evacuation: Decision-making and life safety, Transportation Research Part C: Emerging Technologies 64 (2016) 86–100.
[16] Z. Wang, G. Jia, Sensitivity Analysis of Tsunami Evacuation Risk with Respect to Epistemic Uncertainty, ASCE-ASME Journal of Risk and Uncertainty in Engineering Systems, Part A: Civil Engineering 8 (3) (2022) 04022037.
[17] A. Muhammad, R. De Risi, F. De Luca, N. Mori, T. Yasuda, K. Goda, Are current tsunami evacuation approaches safe enough? Stoch. Environ. Res. Risk Assess. 35 (4) (2021) 759–779.
[18] Central Disaster Management Council 2012. Working Group Report on Mega-Thrust Earthquake Models for the Nankai Trough, Japan. Cabinet Office of the Japanese Government, Tokyo, http://www.bousai.go.jp/jishin/nankai/nankaitrough_info.html.
[19] K. Goda, R. De Risi, Multi-hazard loss estimation for shaking and tsunami using stochastic rupture sources, Int. J. Disaster Risk Reduc. 28 (2018) 539–554.
[20] Central Disaster Management Council, Working Group Report on Mega-Thrust Earthquake Models for the Nankai Trough, Japan. Cabinet Office of the Japanese Government, Tokyo, 2012. http://www.bousai.go.jp/jishin/nankai/nankaitrough_info.html.
[21] K. Goda, P.M. Mai, T. Yasuda, N. Mori, Sensitivity of tsunami wave profiles and inundation simulations to earthquake slip and fault geometry for the 2011 Tohoku earthquake, Earth Planets Space 66 (1) (2014) 1–20.
[22] K. Goda, T. Yasuda, N. Mori, T. Maruyama, New scaling relationships of earthquake source parameters for stochastic tsunami simulation, Coast Eng. J. 58 (3) (2016) 1650010–1650011.
[23] A. Muhammad, K. Goda, Impact of earthquake source complexity and land elevation data resolution on tsunami hazard assessment and fatality estimation, Comput. Geosci. 112 (2018) 83–100.
[24] F. Hirose, K. Maeda, K. Fujita, A. Kobayashi, Simulation of great earthquakes along the Nankai Trough: reproduction of event history, slip areas of the Showa Tonankai and Nankai earthquakes, heterogeneous slip-deficit rates, and long-term slow slip events, Earth Planets Space 74 (1) (2022) 1–31.
[25] P.M. Mai, K.K.S. Thingbaijam, SRCMOD: an online database of finite-fault rupture models, Seismol Res. Lett. 85 (6) (2014) 1348–1357.
[26] R. De Risi, K. Goda, Simulation-based probabilistic tsunami hazard analysis: empirical and robust hazard predictions, Pure Appl. Geophys. 174 (8) (2017) 3083–3106.
[27] Y. Okada, Surface deformation due to shear and tensile faults in a half-space, Bull. Seismol. Soc. Am. 75 (4) (1985) 1135–1154.
[28] Y. Tanioka, K. Satake, Tsunami generation by horizontal displacement of ocean bottom, Geophys. Res. Lett. 23 (8) (1996) 861–864.
[29] C. Goto, Y. Ogawa, N. Shuto, F. Imamura, Numerical method of tsunami simulation with the leap-frog scheme, IOC Manuals and Guides 35 (1997) 130.
[30] R. Akoh, T. Ishikawa, T. Kojima, M. Tomaru, S. Maeno, High-resolution modeling of tsunami run-up flooding: a case study of flooding in Kamaishi city, Japan, induced by the 2011 Tohoku tsunami, Nat. Hazards Earth Syst. Sci. 17 (11) (2017) 1871–1883.
[31] M. Balmer, M. Rieser, K. Meister, D. Charypar, N. Lefebvre, K. Nagel, MATSim-T: architecture and simulation times, in: Multi-agent Systems for Traffic and Transportation Engineering, IGI Global, 2009, pp. 57–78.
[32] A. Horni, K. Nagel, K.W. Axhausen (Eds.), The Multi-Agent Transport Simulation MATSim, Ubiquity Press, London, 2016, p. 618.
[33] M.D. Mauro, M. Lees, K. Megawati, Z. Huang, Pedestrian-vehicles interaction during evacuation: agent-based hybrid evacuation modelling of Southeast Asian cities, in: Pedestrian and Evacuation Dynamics 2012, Springer, Cham, 2014, pp. 435–443.
[34] W. Tobler, Three Presentations on Geographical Analysis and Modeling. Non-isotropic Geographic Modeling: Speculations on the Geometry of Geography, and Global Spatial 634 Analysis, Technical report (National Center for Geographic Information Analysis. NC- 635 GIA. (National Center for Geographic Information and Analysis). Available at: 636, 1993. www.ncgia.ucsb.edu/Publications/Tech_Reports/93/93-1.
[35] T. Sugimoto, H. Murakami, Y. Kozuki, K. Nishikawa, T. Shimada, A human damage prediction method for tsunami disasters incorporating evacuation activities, Nat. Hazards 29 (3) (2003) 587–602.
[36] N.Y. Yun, M. Hamada, Evacuation behavior and fatality rate during the 2011 Tohoku-Oki earthquake and tsunami, Earthq. Spectra 31 (3) (2015) 1237–1265.
[37] C. Caliendo, P. Ciambelli, M.L. De Guglielmo, M.G. Meo, P. Russo, Simulation of people evacuation in the event of a road tunnel fire, Procedia-social and behavioral sciences 53 (2012) 178–188.
[38] H. Chu, J. Yu, J. Wen, M. Yi, Y. Chen, Emergency evacuation simulation and management optimization in urban residential communities, Sustainability 11 (3) (2019) 795.
[39] E. Mas, A. Suppasri, F. Imamura, S. Koshimura, Agent-based simulation of the 2011 great east japan earthquake/tsunami evacuation: an integrated model of tsunami inundation and evacuation, J. Nat. Disaster Sci. 34 (1) (2012) 41–57.
[40] M. Pregnolato, A. Ford, S.M. Wilkinson, R.J. Dawson, The impact of flooding on road transport: a depth-disruption function, Transport. Res. Transport Environ. 55 (2017) 67–81.